Molecular Microbiology (2001) **40**(4), 976–990

Repression of virulence genes by phosphorylation-dependent oligomerization of CsrR at target promoters in *S. pyogenes*

Alita A. Miller,[1,2] N. Cary Engleberg[1,3] and Victor J. DiRita[1,2]*

[1]*Department of Microbiology and Immunology,*
[2]*Unit for Laboratory Animal Medicine, and*
[3]*Department of Internal Medicine, 5641 Medical Science II, University of Michigan Medical School, Ann Arbor, MI 48109, USA.*

Summary

csrRS **encodes a two-component regulatory system that represses the transcription of a number of virulence factors in** ***Streptococcus pyogenes*****, including the hyaluronic acid capsule and pyrogenic exotoxin B. CsrRS-regulated virulence factors have diverse functions during pathogenesis and are differentially expressed throughout growth. This suggests that multiple signals induce CsrRS-mediated gene regulation, or that regulated genes respond differently to CsrR, or both. As a first step in dissecting the** ***csrRS*** **signal transduction pathway, we determined the mechanism by which CsrR mediates the repression of its target promoters. We found that phosphorylated CsrR binds directly to all but one of the promoters of its regulated genes, with different affinities. Phosphorylation of CsrR enhances both oligomerization and DNA binding. We defined the binding site of CsrR at each of the regulated promoters using DNase I and hydroxyl radical footprinting. Based on these results, we propose a model for differential regulation by CsrRS.**

Introduction

The Gram-positive bacterium *Streptococcus pyogenes* (group A *Streptococcus* or GAS) is an important and versatile human pathogen that possesses a complex array of precisely regulated virulence factors. GAS is capable of prospering in multiple environments: infection is seen at many levels, ranging from mild, self-contained infections of skin and mucous membranes (in diseases such as impetigo and pharyngitis) to deep, invasive infections of the muscles, lungs and bloodstream (resulting in much more serious diseases such as cellulitis, necrotizing fasciitis and toxic shock). Within the large and complex arsenal of virulence factors found in GAS are (i) proteins that cause damage to the host, such as hyaluronidase, streptolysins and pyrogenic exotoxins; (ii) factors that promote adherence and colonization, such as M protein and protein F; and (iii) components that enhance resistance to phagocytosis by the host immune system, such as C5a peptidase, M protein and the hyaluronic acid capsule (for reviews, see Alouf and Muller-Alouf, 1996; Schlievert *et al*., 1996; Cunningham, 2000). During infection, GAS must be able to sense and respond to a given microenvironment by expressing only those virulence factors that are required for infection at that particular site. The ability to regulate a wide range of virulence factors differentially is therefore paramount to the success of GAS infections.

Understanding the pathogenic mechanisms by which this organism causes disease is of fundamental importance, particularly in view of a recently observed rise in the number of severe, invasive infections resulting from GAS (Stevens, 1992; Feingold and Weinburg, 1996; Kaplan, 1996; Schlievert *et al*., 1996). Several virulence regulatory systems have been defined in GAS to date (Caparon and Scott, 1987; Fogg *et al*., 1994; Podbielski *et al*., 1996; 1999a; Chaussee *et al*., 1999; Li *et al*., 1999; McIver *et al*., 1999). CsrRS was initially identified as a negative regulator of hyaluronic acid capsule synthesis genes (*hasAB*) resulting from the generation of hypermucoid colonies upon Tn*916* transposition (Levin and Wessels, 1998; Heath *et al*., 1999) or targeted mutation of genes with homology to *phoPQ*, which encodes a regulator of virulence in invasive *Salmonella* species (Federle *et al*., 1999). CsrRS belongs to the two-component system family of signal transduction pathways (for a review, see Hoch and Silhavy, 1995). In these systems, the extracellular domain of a membrane-spanning sensor kinase (CsrS) receives a stimulus that results in autophosphorylation of an intracellular domain on a conserved histidine residue. The phosphate group is transferred to a cytoplasmic effector protein (CsrR), which often regulates transcription directly or indirectly.

In addition to capsule production (*hasAB*), CsrRS negatively regulates the expression of the pyrogenic

Accepted 12 March, 2001. *For correspondence at the Department of Microbiology and Immunology. E-mail vdirita@umich.edu; Tel. (+1) 734 936 3804; Fax (+1) 734 936 3235.

exotoxin B (*speB*), the streptolysin S-associated gene (*sagA*), streptokinase (*ska*), mitogenic factor (*speMF*) and its own transcription (Federle *et al*., 1999; Heath *et al*., 1999). CsrRS-regulated genes are expressed differentially throughout growth: maximal levels of *hasAB* expression are seen during exponential phase, whereas secreted proteins, such as pyrogenic exotoxin B, mitogenic factor and streptolysin S, are maximally expressed during stationary phase (Federle *et al*., 1999; Unnikrishnan *et al*., 1999). These CsrRS-repressed genes encode products with significantly diverse pathogenic functions. Hyaluronic acid capsule plays a major role in protecting the organism from phagocytosis (Wessels and Bronze, 1994; Moses *et al*., 1997). SpeMF is a pyrogenic exotoxin that acts as a superantigen (Yutsudo *et al*., 1992) and has recently been shown to possess DNase activity (Sriskandan *et al*., 2000). Both streptokinase, a plasminogen-binding and -activating protein (Lottenberg *et al*., 1992), and streptolysin S, a highly active cytolysin (Alouf and Loridan, 1988; Betschel *et al*., 1998), appear to play a role in bacterial spread and tissue invasion. Another CsrRS-controlled gene that may be involved in bacterial spread is *speB*, which encodes a potent cysteine protease that cleaves both host and streptococcal proteins (Chaussee *et al*., 1993; Ohara-Nemoto *et al*., 1994; Musser *et al*., 1996). In spite of the demonstration *in vitro* of numerous, potentially important functions of SpeB, there are conflicting reports about the contribution of this protease to disease in mouse models (Lukomski *et al*., 1997; Ashbaugh *et al*., 1998; Kuo *et al*., 1998).

As CsrRS-regulated genes are both differentially regulated and contribute to the pathogenesis of GAS in different ways, it is clearly important to understand the mechanism(s) by which control is mediated in response to environmental signals. In many homologous two-component systems, modulation of transcription is directly dependent on both the intracellular concentration and the phosphorylation state of the response regulator (for examples, see Forst *et al*., 1989; Galinier *et al*., 1994; Karimova *et al*., 1996; Dahl *et al*., 1997). This is also likely to be the case for CsrR; it is notably capable of autoregulation (Federle *et al*., 1999; A. A. Miller and V. J. DiRita, unpublished results), and its phosphorylation state is probably modulated by CsrS in response to environmental signals. Determining the nature of the interaction between CsrR and its target promoters is a crucial first step in understanding the CsrRS signalling pathway. Bernish and van de Rijn (1999) recently showed that phosphorylated CsrR binds directly to a large, AT-rich stretch of *hasAB* promoter DNA containing the −35 and −10 regions as well as up to 67 bp into the coding region. In spite of these observations, no consensus binding sequence is discernible upon comparison of all the different putative promoters of *csrRS*-regulated genes.

In this study, we define the mode of interaction of CsrR with its other target promoters in order to begin to understand how CsrRS differentially regulates a number of genes. We present evidence that phosphorylated CsrR binds as an oligomer to large stretches of AT-rich promoter DNA and that phosphorylation of the protein enhances both its oligomerization and its DNA binding. We propose a model in which both the protein concentration and the phosphorylation state of CsrR at a given time during cell growth and/or infection are responsible for the repression of multiple virulence factors in GAS.

Results

Mapping of the transcription start site of CsrRS-regulated genes in MGAS166

Although CsrRS-regulated genes have putative −35 and −10 promoter elements with apparent homology to σ^{70} promoter consensus sequences, the only transcription start site that has been experimentally defined is that of p_{hasA} (Dougherty and van de Rijn, 1994). In order to analyse the interaction between CsrR and the promoters of other genes that it regulates, it was therefore necessary to map precisely the start site of transcription for each of them.

We performed primer extension analysis on samples taken from wild-type and $\Delta csrRS^{-}$ GAS strains at four different times throughout the growth curve (Fig. 1). Expression of *hasAB* and *csrRS* is maximal during early and mid-exponential growth, whereas *speB* and *speMF* are maximally expressed during stationary phase. These expression patterns remain the same, although greatly enhanced, in the $\Delta csrRS^{-}$ strain. We observed a gradual increase in expression of both *sagA* and *ska* throughout growth, which is also significantly greater in the mutant strain. These data confirm and extend previous observations on the relative transcription levels of CsrRS-regulated genes in wild-type and mutant *csrRS* backgrounds (Federle *et al*., 1999; Unnikrishnan *et al*., 1999), although Federle *et al*. (1999) saw no CsrRS-mediated regulation of *speB* in their strain background. Taken together, these data suggest that CsrRS represses multiple virulence factors at different times throughout the growth phase.

To determine the transcription start site for each promoter, we compared the size of the primer extension products with DNA sequencing ladders that were obtained by semi-exponential cycle sequencing as described in *Experimental procedures*. With the exception of *speB*, promoter elements for each gene map to within 200 nucleotides of the putative translation initiation sites of each of the CsrRS-regulated genes (Fig. 2). We mapped the *speB* promoter to a position 1070 nucleotides

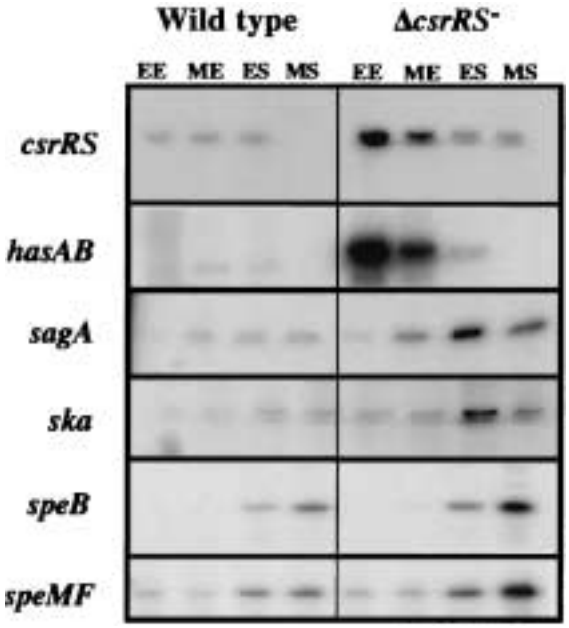

Fig. 1. *csrRS* represses many genes at different times throughout growth. Primer extension analysis was performed to map the start site of transcription (see Fig. 2) and to determine RNA levels as a function of growth phase in wild-type and mutant (*ΔcsrRS*$^-$) strains. EE, early exponential; ME, mid-exponential; ES, early stationary; MS, mid-stationary phases. The same RNA samples were used for analysis with all probes. Note that a *csrR* transcript can be detected in the *ΔcsrRS*$^-$ strain because it contains an internal deletion in the *csrR* coding region (with an intact promoter). Primers for each gene were chosen with two criteria in mind: (i) their relative location to the putative −35 and −10 sites; and (ii) minimization of the degree of AT-rich sequence in order to optimize annealing of the oligonucleotide.

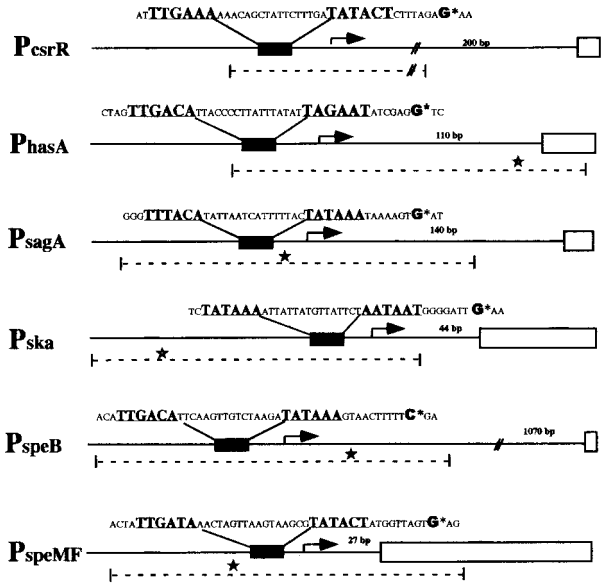

Fig. 2. Transcription start sites for *csrRS*-regulated genes. Primer extension analysis was performed on RNAs isolated from wild-type or mutant (*ΔcsrRS*$^-$) strains (see Fig. 1), and the products of these reactions were compared with DNA sequencing ladders generated by semi-exponential cycle sequencing (not shown). Black boxes correspond to the sequences containing promoter elements through the start site of transcription. White boxes represent coding sequences. Promoter sequences are underlined, and the start site of transcription for each promoter is denoted by an asterisk in the sequence and an arrow in the figure. The sequences used for probes in EMSA and footprinting analyses are indicated by a dashed line. A 15 bp conserved motif (defined in Fig. 6) is indicated by a star.

upstream of the SpeB translation start site. Two *speB* transcripts (2.1 and 1.7 kb) are detected upon Northern analysis (Lyon *et al*., 1998; Heath *et al*., 1999), and it has been proposed that *speB* may be regulated by multiple promoters (Lyon *et al*., 1998). We therefore analysed *speB* promoter activity by primer extension using five additional probes, each of which was ≈200 bp downstream of the next. We detected no additional transcription start site beyond that found at −1070 (data not shown). There are five putative small open reading frames (ORFs) between the promoter elements and the SpeB start codon, which would give rise to proteins ranging in size from 25 to 56 amino acids. Transcription initiation from the promoter at −1070 would give rise to a 2.1 kb transcript (assuming that *speB* is the last gene transcribed), corresponding exactly to the size of the larger band obtained by Northern analysis.

CsrR binds directly and specifically to promoter sequences of all but one CsrRS-regulated gene

The next step in our analysis was to determine whether or not CsrR binds directly to the promoters of each of its target genes. For these studies, we generated a *his$_6$-csrR* clone that was used to produce large quantities of his$_6$-CsrR purified from overexpression in *Escherichia coli*. We tested both non-phosphorylated and phosphorylated forms of the highly purified (> 95%) his$_6$-CsrR for their ability to bind to a 200 bp end-labelled polymerase chain reaction (PCR) fragment containing *hasA* promoter DNA (depicted by dashed line in Fig. 2). This sequence has been shown previously to interact directly with CsrR (Bernish and van de Rijn, 1999). Both phosphorylated and non-phosphorylated his$_6$-CsrR formed complexes with *hasA* promoter DNA, and the mobility of the resulting complex decreased as protein concentration was increased (Fig. 3). In addition, we found that the non-phosphorylated his$_6$-CsrR–promoter complexes migrated notably faster than phosphorylated his$_6$-CsrR–promoter complexes when equivalent amounts of protein were used (compare 3 and 6 μM for both). These data suggest that there are multiple CsrR binding sites on the promoter DNA that are bound more efficiently by phosphorylated CsrR. Alternatively, the decrease in mobility could result from the sequential binding of additional his$_6$-CsrR

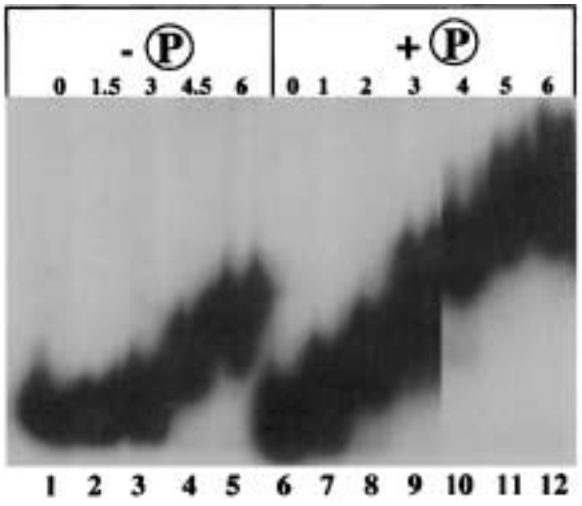

Fig. 3. Purified his_6-CsrR binds to *hasA* promoter DNA. EMSAs were performed on a labelled PCR fragment containing p_{hasA} with increasing amounts (1–6 μM) of either non-phosphorylated (lanes 2–5) or phosphorylated (lanes 7–12) his_6-CsrR. Lanes 1 and 6 are labelled probe alone.

molecules to those that initially bound to the DNA. The latter explanation would suggest that phosphorylation of CsrR increases the ability of the protein to self-associate.

We next tested the ability of his_6-CsrR to interact with CsrRS-regulated promoters (as defined in Fig. 2; probes used are shown as dashed lines). Our negative control was the promoter for the *ctxA* gene of *Vibrio cholerae*, which, like the CsrRS-regulated promoters from GAS, is rich in AT sequences. As shown in Fig. 4, phosphorylated his_6-CsrR (his_6-CsrR-P) bound directly to all the promoters of CsrR-repressed genes except its own. Because the CsrR footprint on the *hasA* promoter was found to extend into the coding sequence (Bernish and van de Rijn, 1999), we speculated that CsrR may bind to *csrR* DNA at sequences further downstream than those present in the fragment used in the experiment in Fig. 4. Two other probes of downstream DNA (≈300 bp in size), encompassing the entire coding region, were tested for CsrR binding, but neither was able to bind to his_6-CsrR-P (data not shown). These results suggest that *csrRS* autoregulation occurs indirectly, apparently involving other factors. Another possibility is that sequences further upstream of −95 (the end-point of the first p_{csrR} probe tested) contain the CsrR binding site and somehow mediate negative autoregulation.

In agreement with the results shown for p_{hasA} (Fig. 3), increasing amounts of his_6-CsrR-P resulted in decreasing mobility of the other promoter–CsrR-P complexes. Lower concentrations of CsrR were required for a mobility shift to occur with p_{ska} and p_{speMF} than those required for shifting with p_{speB}, p_{sagA} and p_{hasA}, suggesting that CsrR has greater affinity for p_{ska} and p_{speMF}. Very small shifts were

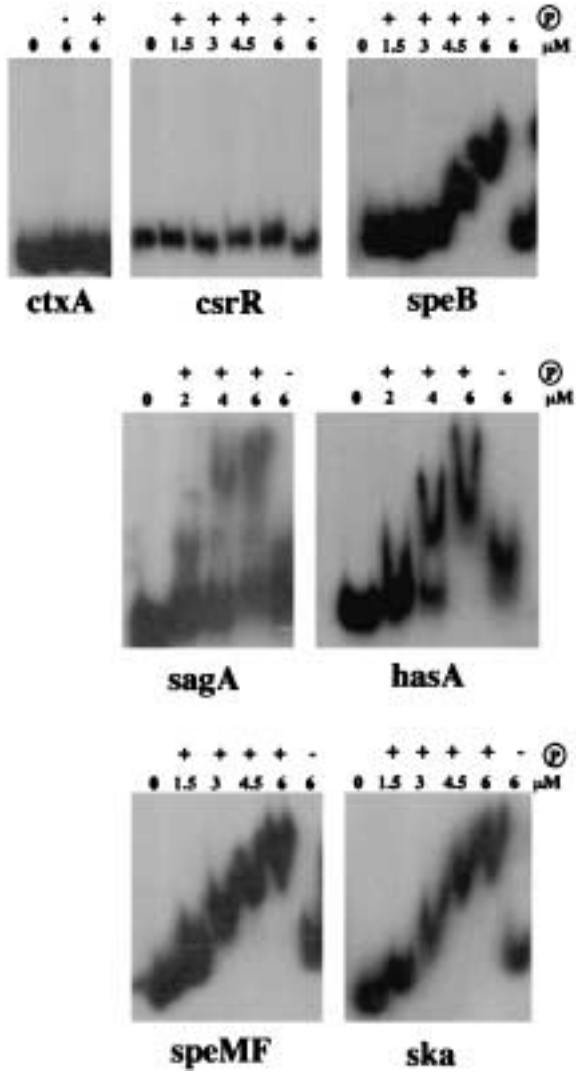

Fig. 4. CsrR binds directly to all but one of its target promoters. The interaction between CsrR and target promoters was analysed by EMSA. Increasing amounts of phosophorylated his_6-CsrR were incubated with labelled PCR fragments containing different promoter DNA sequences as indicated. In comparison, the maximum amount of his_6-CsrR (6 μM) was tested for its ability to bind to DNA in the absence of phosphorylation (last lane in each panel). The first lane in each panel is the labelled DNA probe alone. The negative control was the AT-rich promoter for the *ctxA* gene of *Vibrio cholerae*.

observed upon incubation of non-phosphorylated his_6-CsrR with p_{speB}, p_{sagA} and p_{hasA}, whereas slightly more binding of non-phosphorylated protein occurred with p_{ska} and p_{speMF}. Notably, phosphorylation of his_6-CsrR markedly increased the size of protein–DNA complex for each of the promoters (compare the last two lanes in each gel). In addition, the size of the his_6-CsrR-P–DNA complex differed depending on the probe. Complexes formed by his_6-CsrR-P with p_{sagA}, p_{speB} and p_{hasA} migrated faster than those formed with p_{ska} and p_{speMF}. Therefore, we conclude that promoters for which CsrR has lower affinity

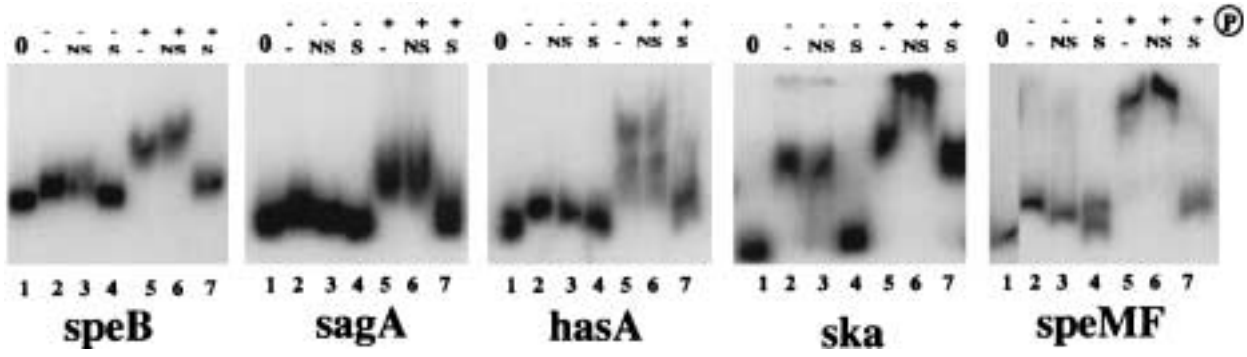

Fig. 5. Binding by CsrR to its target promoters is specific. EMSAs were performed with 6 μM of either non-phosphorylated (lanes 2–4) or phosphorylated (lanes 5–7) his_6-CsrR in the presence of unlabelled non-specific (p_{ctxA}, labelled as NS) (lanes 3 and 6) or specific (same as probe, labelled as S) (lanes 4 and 7) competitor DNA (at 100-fold excess). Lane 1 is the labelled DNA probe alone.

generally also form smaller sized complexes with his_6-CsrR-P. Because all the probes are approximately the same size, the differences in mobility between different promoters could indicate the presence of more CsrR binding sites or sites with higher affinity (or both) in those promoters that form the slowest migrating complexes. Other possibilities are (i) that the site of binding of CsrR differs between probes, i.e. the mobility of the complex of a protein bound at the end of a DNA fragment may be different than if it bound in the middle; or (ii) that CsrR binding induces DNA bending, giving rise to structures that vary among the promoters and migrate differentially during electrophoretic mobility shift assays (EMSAs) (Wu and Crothers, 1984).

To test the specificity of the CsrR–promoter interactions, non-specific (p_{ctxA}) or specific (same as probe) unlabelled competitor DNA was incubated with his_6-CsrR or his_6-CsrR-P before the addition of radiolabelled probe (Fig. 5). These experiments resulted in two general types of behaviours for the six different probes, which probably reflects the differences in affinity of CsrR and CsrR-P for each promoter. Non-specific unlabelled DNA competed poorly for complex formation of either his_6-CsrR or his_6-CsrR-P with any of the probes tested (see Fig. 5, lanes 3 and 6 of each blot). The addition of specific unlabelled DNA completely abrogated binding by either his_6-CsrR or his_6-CsrR-P to radiolabelled p_{hasA}, p_{sagA} and p_{speB} (see Fig. 5, lanes 4 and 7). These are the promoters that appear to have fewer CsrR binding sites or binding sites with lower affinity for CsrR, as shown in Fig. 4. In contrast, the addition of specific unlabelled DNA to complexes containing CsrR and p_{ska} or p_{speMF} resulted in species that retained a mobility that corresponds to the complex formed with non-phosphorylated his_6-CsrR (see Fig. 5, lane 7), for reasons which remain unclear. These are the promoters that appear to have greater affinity and/or contain more CsrR binding sites. Taken together, these data demonstrate the specificity of CsrR binding to its target promoters and suggest that there may be fundamental differences in the way in which CsrR forms complexes with the two groups of promoters: those binding with lower affinity leading to smaller complex formation (p_{hasA}, p_{sagA} and p_{speB}) and those binding with higher affinity forming larger complexes (p_{ska} or p_{speMF}).

CsrR binds to promoter DNA as an oligomer

The above results show that CsrR binds directly and specifically to target promoters. However, no consensus that could serve as the CsrR binding site was found in these promoters upon comparison of their DNA sequences, although they are all notably AT rich (ranging from 66% to 77%; see Table 1). We therefore performed footprinting analysis on CsrR–DNA complexes in order to define precisely the CsrR binding site at each of the promoters. The DNA probes used for these experiments are the same as those used for EMSA (shown as dashed lines in Fig. 2), except that the DNA was end labelled only on the template strand. As shown in Fig. 6, his_6-CsrR binding resulted in a large DNase I footprint on target promoters that surrounded the −35 and −10 sequences, whose size and/or intensity increased when the protein was phosphorylated (Fig. 6, lanes 2–4 in each blot). Based on the sequencing ladder that was run alongside each footprinting reaction, we defined the boundaries of each DNase I footprint for promoters bound by his_6-CsrR-P (depicted as a solid line in Fig. 6 and summarized in Table 1), with the average footprint measuring ≈ 110 bp.

Because analysis by DNase I footprinting can be limited as a result of the tendency of the enzyme to cleave at only a subset of positions, especially in AT-rich DNA (Drew and Travers, 1984), we reasoned that the CsrR binding site could be defined more clearly using hydroxyl radical ($OH^{\bullet}$) footprinting, which cleaves the DNA backbone at every base (Tulius *et al.*, 1987). This analysis gave rise to striking footprints, demonstrating that his_6-CsrR protects

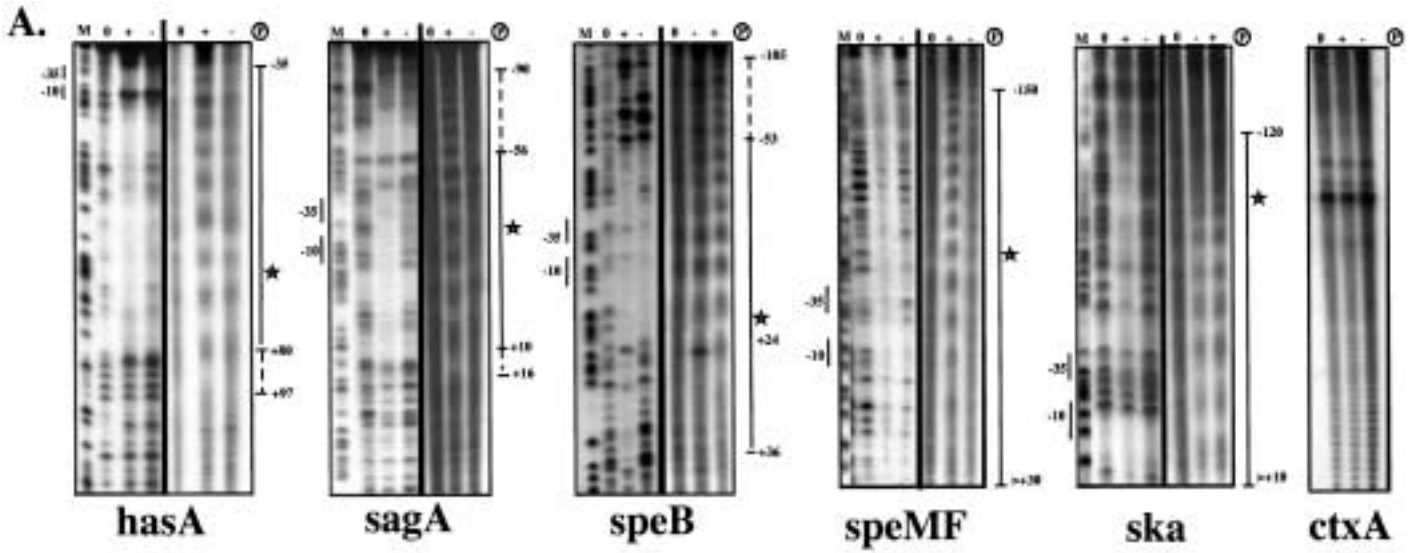

B.

promoter	sequence (5'-3')	location
hasA	-TATTTTTAAAAAAAC	+55 to +70
sagA	TCATTTTTACTATAAA	-25 to -10
speB	TTATTTTTAATAAAAC	+22 to +31
speMF	TATTTTTTAAAAAAAC	-52 to -37
ska	-TATTATTAAAAACAA	-74 to -61
consensus	$T\frac{T}{A}ATTTTTAA\frac{A}{T}AAAA\frac{C}{A}$	

Fig. 6. Definition of CsrR binding sites by DNase I and $OH^{\bullet}$ footprinting.
A. DNase I (left) and hydroxy radical (right) footprinting analyses were performed on complexes formed between radiolabelled promoter DNA and his_6-CsrR (lanes marked –) or his_6-CsrR-P (lanes marked +) and compared with digestion patterns of the DNA probe alone (lanes marked 0). Sequencing ladders were run for comparison (M). Promoter elements are indicated on the left. The DNase I footprint is depicted with a solid line to the right; where appropriate, the extended $OH^{\bullet}$ footprint is shown with a dashed line. All footprinting results are summarized in Table 1.
B. Sequence and location of the 15 bp conserved motif [indicated in (A) and in Fig. 2 by a star].

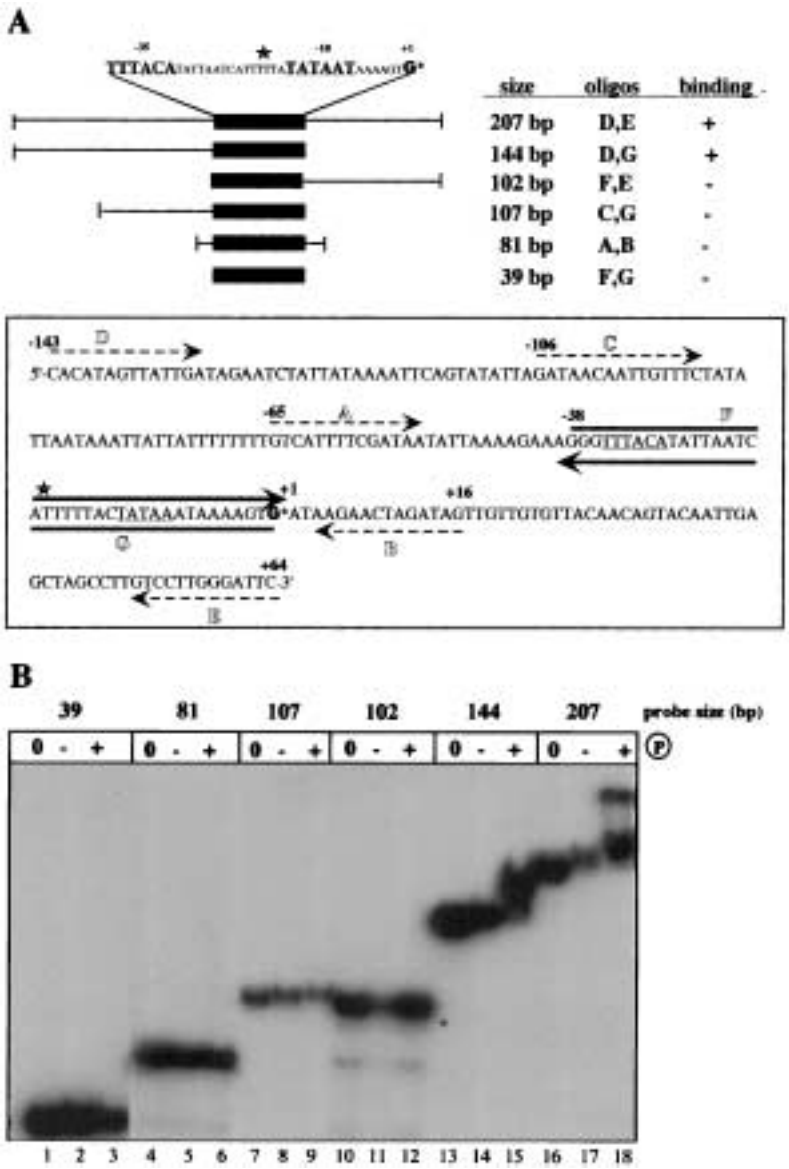

Fig. 7. Definition of a minimal CsrR binding site at p_{sagA}.
A. Various sized DNA fragments containing different regions of the DNA sequences around p_{sagA} were generated by PCR using the indicated oligomers (except for the 39-mer, which was made by annealing two complementary oligomers), purified and end labelled. Note that the 39-mer probe contains the −35 and −10 region and is shown by a heavy arrow; the 'conserved motif' shown in Fig. 6 is marked by a star.
B. EMSAs were performed on DNA fragments depicted in (A) with 6 μM non-phosphorylated (lanes marked –) or phosphorylated (lanes marked +) his_6-CsrR. Lanes marked 0 are labelled probe alone.

large stretches of DNA at its target promoters (Fig. 6, lanes 5–7). The periodicity of the footprinting pattern indicates that CsrR bound predominantly on one face of the DNA helix. The $OH^{\bullet}$ footprints (summarized in Table 1) map to the same regions on the DNA as the DNase I footprints, although they are larger for most of the probes (shown as a dashed line), averaging ≈ 130 bp in size.

The intensity and size of the footprints for both non-phosphorylated and phosphorylated his_6-CsrR appear to vary somewhat depending on the promoter fragment, irrespective of the method used. To demonstrate the accuracy of the footprinting analysis, we performed both DNase I and $OH^{\bullet}$ footprinting on the complementary strand of the p_{sagA} promoter. As expected, the footprints observed on this strand correspond well to those seen on the template strand (data not shown).

Although much less intense, the general pattern of $OH^{\bullet}$ footprint is the same for non-phosphorylated versus phosphorylated his_6-CsrR, suggesting that the binding of CsrR to promoter DNA is the same irrespective

Table 1. Summary of footprinting results.

Promoter	% AT	DNase I footprint	Size (bp)	$OH^{\bullet}$ footprint	Size (bp)
sagA	77.0	−56 to +10	66	−90 to +16	106
speB	72.7	−53 to +36	88	−105 to +24	129
hasA	73.0	−35 to +80	115	−35 to +97	132
ska	73.8	−120 to > +10	> 130	−120 to > +10	> 130
speMF	66.3	−150 to > +30	> 180	−150 to > +30	> 180

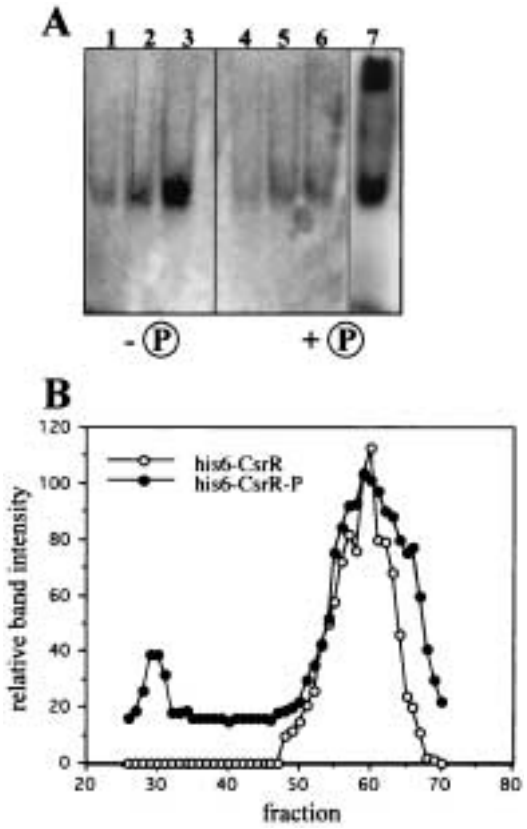

Fig. 8. Phosphorylation of CsrR results in self-association.
A. Phosphorylation-dependent CsrR self-association was analysed by incubation of increasing amounts (0.6, 1.2 and 2.4 μg) of his_6-CsrR in the absence (lanes 1–3) or presence (lane 4–6) of acetyl phosphate and subsequent analysis by 8% native gel electrophoresis. To trace the phosphate moiety during these reactions, 2.4 μg of his_6-CsrR was incubated with radiolabelled acetyl phosphate and analysed similarly (lane 7).
B. Samples of 150 μg of phosphorylated or non-phosphorylated his_6-CsrR (in 200 μl total volume) were analysed by gel filtration on a Biogel A-0.2M column. Fractions were analysed by SDS–PAGE (not shown). His_6-CsrR bands were quantified and plotted against elution time.

of its phosphorylation state; we surmise that the interaction becomes more stable upon phosphorylation. However, results from Figs 4 and 5 suggest that the complexes formed between CsrR and promoter DNA differ significantly in their size upon phosphorylation. Based on these observations, we hypothesize that the mobility shift differences in the EMSA may reflect not only CsrR–DNA interactions, but also CsrR–CsrR interactions, i.e. that his_6-CsrR self-associates upon phosphorylation. This would result in complexes in which some of the CsrR molecules are binding only to other CsrR molecules and not directly to the promoter DNA, which could explain the differences observed in EMSA and footprinting analysis. This hypothesis is tested below.

Productive binding of CsrR requires long segments of AT-rich DNA

The above results suggest that CsrR binds large regions of target promoter DNA, but do not give any indication of the minimal binding site necessary for CsrR binding. Comparison of the CsrR footprints revealed that the most common feature among these promoter sequences is the high degree of AT-rich DNA, most notably runs of As or Ts. Upon close inspection, we identified one 16 bp motif, 5′-T(T/A)ATTTTAA(A/T)AAAA(C/A)-3′, which was conserved among all five promoter sequences but whose placement with respect to the promoter elements appeared to vary randomly (indicated by a star in Figs 2, 6A and 7; sequences and locations shown in Fig. 6B). In order to determine how often this motif occurs within the genome, we performed a BLASTN search of the MGAS166 (M1) strain (available at http://dna1.chem.ou .edu/strep.html). Using all eight variants of the consensus sequence, we obtained a total of 13 positive hits (with 15 out of the16 bases matching). This number is well above the random occurrence of a given 16-mer in the genome. Owing to this frequency of occurrence and its conservation in CsrR-regulated promoters, we hypothesized that this motif may play a role in specific recognition by CsrR of its target promoters.

We addressed this hypothesis in two ways. First, we attempted to define a minimal CsrR binding site by titrating our footprinting experiments with decreasing amounts of his_6-CsrR-P, reasoning that the bands of intermediate mobility observed in EMSA for P_{hasA} and P_{sagA} represent the interaction of CsrR-P to a minimal, or nucleation, binding site. However, instead of seeing a reduction in the footprint size as the his_6-CsrR-P concentration was decreased, we found that the size of the first detectable footprints corresponded exactly to those shown in Fig. 6A (data not shown). This implies that the binding of CsrR to its target promoters is co-operative as protein concentration increases. However, these results do not exclude the possibility that a higher affinity site exists for CsrR: the transition from lower to higher ordered interactions with promoter DNA could simply be too rapid to detect by this method.

Our second test of the above hypothesis involved determining the CsrR binding affinity for different subsets of the *sagA* promoter (summarized in Fig. 7). The *sagA* promoter appears to bind fewer CsrR molecules relative to the other promoters, as determined by EMSA (see Fig. 4), and has the smallest footprint for CsrR-P (see Fig. 6A and Table 1); hence, determination of a minimal binding site on this promoter would theoretically be the most straightforward. The conserved 15 bp motif is located at −25 to −10 in p_{sagA}. EMSA showed that his_6-CsrR-P was unable to bind to probes either 39 or

81 bp in length that contained this conserved motif and promoter elements, regions that were clearly protected by CsrR in our footprinting analyses (Fig. 7B, lanes 1–6). In addition, neither a 102 bp fragment with the −35 box located at the 5′ end (from −38 to +64; Fig. 7B, lanes 7–9) nor a 107 bp fragment containing sequences from −106 to + 1 (Fig. 7B, lanes 10–12) were bound by his_6-CsrR-P. However, his_6-CsrR-P did bind to a 144 bp probe with a downstream end-point of +1 and an upstream end-point of −143 (Fig. 7B, lanes 13–15). The additional bases in this probe are not protected in the footprinting experiments; thus, we reason that it is not likely that a nucleation site for CsrR binding resides in this stretch of DNA (from −143 to −106).

Because all these probes contain the CsrR binding site, as defined by footprinting, we speculate that CsrR recognition of its target promoters requires not only AT-rich DNA, but that substantially long regions (> 100 bp) of DNA containing these sites must be present for its stable and productive binding. In addition, the role (if any) of the conserved motif is unclear: although it may contribute to the recognition of target promoters by CsrR, it is certainly not sufficient to mediate CsrR binding to DNA.

Phosphorylation induces oligomerization of CsrR in the absence of DNA

The EMSA data show that phosphorylation of CsrR results in higher ordered protein–DNA complexes, whereas footprinting data suggest that phosphorylation of CsrR leads to more stable DNA–protein interactions. Taken together, these results imply that phosphorylation causes a conformational change in CsrR, allowing for self-association of the protein and stable interaction with promoter DNA. To test the effect of phosphorylation on CsrR in the absence of DNA, we analysed the relative mass of phosphorylated and non-phosphorylated his_6-CsrR. Coomassie staining showed that non-phosphorylated his_6-CsrR runs as a low-molecular-weight species on native gels, even as protein concentration is increased (Fig. 8A, lanes 1–3); upon phosphorylation, the intensity of the band corresponding to this species is greatly reduced, and higher molecular weight species are observed (Fig. 8A, lanes 4–6). When his_6-CsrR was incubated with radiolabelled acetyl phosphate and analysed by native gel electrophoresis followed by autoradiography, the majority of the radioactivity migrated at a size corresponding to an oligomerized form of CsrR, although labelled phosphate was also detected in the lower molecular weight form of the protein (Fig. 8A, lane 7). These results imply that phosphorylation (and not increasing concentrations) of CsrR causes it to self-associate.

To determine the size and relative amount of the oligomer in the context of total protein, phosphorylated and non-phosphorylated his_6-CsrR were passed over a gel filtration sizing column that was standardized as described in *Experimental procedures*. SDS–PAGE was performed on individual eluted fractions after trichloroacetic acid (TCA) precipitation, and the relative amount of CsrR in each fraction was determined (Fig. 8B). In the absence of phosphorylation, CsrR eluted as a monomer (≈26 kDa); upon phosphorylation, ≈20% of the total protein migrated as an oligomer of > 200 kDa in size. This ratio is in contrast to that observed in the radiolabelled his_6-CsrR-P experiment, in which the band corresponding to the CsrR-P oligomer predominated. We speculate that this difference (in relative amounts of CsrR-P oligomer) reflects the inefficiency of CsrR autophosphorylation, as the autoradiograph (Fig. 8A, lane 7) only represents the phosphorylated species, whereas the gel filtration analysis (Fig. 8B) accounts for the total protein present in the experiment. Another explanation for the discrepancy between lane 7 of Fig. 8A and B is that the half-life of the phosphorylated form of CsrR is relatively short, which has been documented previously for some other response regulator proteins (Hess *et al*., 1988; Weiss and Magasanik, 1988). Irrespective of these differences, however, the data clearly show that phosphorylation of CsrR is required for the protein to undergo self-association.

Discussion

In many well-characterized two-component regulatory systems, differential modulation of target gene expression is achieved via binding of the response regulator to numerous sites with different affinities and locations within the promoter region. A well-characterized example is the EnvZ/OmpR system, which regulates porin genes in *E. coli* in response to changes in osmolarity. At low osmolarity, low concentrations of phosphorylated OmpR activates transcription of *ompF* by binding to two adjacent sites upstream of its promoter, whereas at higher concentrations (in response to elevated osmolarity), binding to additional lower affinity sites results in repression of *ompF* and activation of *ompC* (reviewed by Egger *et al*., 1997). Another example is the global regulator *bvgAS* found in several *Bordetella* species. Here, the response regulator BvgA functions as both a transcriptional activator of multiple virulence factors and a repressor of genes required for motility and/or survival in response to environmental stimuli such as nicotinic acid and $MgSO_4$ (reviewed by Cotter and DiRita, 2000).

Both OmpR and BvgA have defined binding sites whose strategic placement and relative affinity mediate the choice between transcription activation or repression. Similar to these systems, we have shown that the concentration and phosphorylation state of CsrR regulates its specific affinity for target promoters. What is

unique about CsrR is that it lacks an apparent consensus binding site and, instead, binds as a oligomer to long stretches of AT-rich DNA. In addition, in contrast to other systems, no target promoters have yet been identified in which binding by phosphorylated CsrR leads to transcription activation.

Our data demonstrate that CsrR phosphorylation enhances its binding to long AT-rich sequences, which is shown in terms of both size and intensity of the footprints. We can rule out the possibility that the large size of the footprints simply reflects the aggregation of a purified protein, because CsrR oligomerization in the absence of DNA requires phosphorylation (Fig. 8), yet these footprints occur even when CsrR is not phosphorylated (Fig. 6A). In addition, the location and size of the CsrR-P footprint defined here closely matches that described previously for p_{hasA} (Bernish and van de Rijn, 1999).

Comparison of the CsrR footprints on target promoters shown in Fig. 6A leads to several conclusions. In general, these results are in agreement with conclusions about the degree and affinity of binding, as seen in Figs 4 and 5. For instance, the relative size of the footprints corresponds well with results from EMSA: the promoters that are protected to a greater extent by CsrR are those that form protein–DNA complexes that migrate with a slower mobility in native gels (compare Fig. 4 and Table 1). Note that, for both p_{ska} and p_{speMF}, the 3′ end of the footprint was not precisely defined, as it extends to the end of the probe and may well cover more bases than shown.

Some discrepancies between the results for EMSA and, in particular, the $OH^{\bullet}$ footprinting analysis do exist. Most notable is the fact that the $OH^{\bullet}$ footprint for his_6-CsrR-P is quite large for all the probes, which does not reflect the distinctions between the two promoter classes as defined by EMSA. One explanation for this is that the difference observed in the two types of analyses results from the relative stability of the his_6-CsrR–DNA complex, which may be sufficient to protect the DNA backbone from cleavage during the footprinting reaction, but not to withstand electrophoresis completely in EMSA. In this case, the EMSA data would be more informative in terms of determining the relative binding affinity of CsrR for the different promoters.

Our data show that the phosphorylation of CsrR enhances its ability to self-associate into oligomers (Fig. 8). The role of this oligomerized form of CsrR-P remains to be understood. We hypothesize that relatively weak CsrR–DNA complexes may become more stable after phosphorylation of CsrR, in part because of the subsequent CsrR–CsrR interactions. This interpretation would account for the greater difference seen in mobility between non-phosphorylated and phosphorylated CsrR in Fig. 4 in comparison with the relative size of the footprints for non-phosphorylated versus phosphorylated CsrR shown in Fig. 6A. These data do not rule out the formal possibility that the his_6 tag may somehow contribute to the phosphorylation-dependent oligomerization of CsrR. However, similar footprinting results obtained with non-his_6-tagged CsrR-P at the p_{hasA} promoter (Bernish and van de Rijn, 1999) argue against this.

Although we have observed that the target promoters are AT rich and, in particular, contain runs of uninterrupted As and Ts, we were unable to define a consensus binding site for CsrR. The role of a 15 bp conserved motif (Fig. 6B) in CsrR recognition and DNA binding is unclear, as CsrR was unable to bind to DNA fragments (of less than 144 bp in length) containing this element. In addition, the location of this motif relative to promoter elements is not conserved (see Figs 2 and 6). However, this 15 bp sequence is notably absent in p_{csrRS}, a promoter that, although regulated by CsrRS, is not bound directly by CsrR (Fig. 4).

Given the above, the most pressing question is how CsrR discriminates between the DNA of its target promoters and the rest of the genome, which is also highly AT rich. It is well known that AT-rich DNA has intrinsic bends, and that significant structural discontinuities may arise between the boundaries of poly(A) or (T) tracts and the rest of a nucleotide sequence (Perez-Martin and de Lorenzo, 1997). This suggests that certain secondary structural features may be common to CsrR-regulated promoters and that these may be more important in promoter recognition by CsrR than the primary sequence itself.

The nature of the oligomerized CsrR–DNA interaction is highly reminiscent of that of H-NS, a global transcriptional repressor found in *E. coli* and other enterobacteria, which binds large stretches of intrinsically bent, AT-rich DNA with little primary sequence specificity (reviewed by Williams and Rimsky, 1997; Atlung and Ingmer, 1998). Moreover, oligomerization of H-NS has been shown to be required for specific recognition of bent DNA (Spurio *et al*., 1997). Future experiments may therefore involve defining the region of CsrR required for self-association in order to address the role it plays in DNA binding and repression.

Although we see a difference in CsrR binding to target promoters in terms of (i) the affinity of binding; (ii) the size of the footprint; and (iii) the location of the footprint relative to the −35 and −10 sequences, there is no apparent correlation between CsrR interactions with the different promoters and the timing of their repression, or similarity in their roles in pathogenesis. However, we speculate that differences in affinity observed for the various probes by both non-phosphorylated and phosphorylated CsrR is indeed indicative of the differential regulation that occurs. We therefore suggest a preliminary model for

csrRS-mediated repression of virulence in *S. pyogenes*: the preferential deployment of CsrR at different promoters throughout growth and during infection is a result of both the protein concentration and the degree to which it is phosphorylated, in a precisely defined combination for each promoter. We have observed recently that CsrR protein levels do not remain constant throughout growth and that the protein itself is fairly unstable (A. A. Miller and V. J. DiRita, unpublished results). These results support the notion that rapid and distinct responses (in terms of repression or derepression of certain virulence factors) to specific environmental signals could be precisely controlled through both the phosphorylation state of CsrR as well as the total amount of CsrR protein present in the bacterium.

Finally, it is important to recognize that many of these virulence genes may be regulated at multiple levels. Accordingly, the transcriptional activity of each of these target genes could be a result of CsrRS acting in tandem with other regulators that are not represented in our *in vitro* experiments. For example, one CsrRS-regulated gene, *speB*, has been shown to be activated by both *pel* (Li *et al*., 1999) and *rop* (Lyon *et al*., 1998) and has been proposed to be part of the *mga* regulon (Podbielski *et al*., 1996). Additionally, it is affected by deletions in *rgg* (Chaussee *et al*., 1999) and is known to be upregulated during nutrient deprivation (Chaussee *et al*., 1997; Podbielski *et al*., 1999b) by an as yet undefined mechanism.

In a versatile pathogen such as GAS, global regulators of virulence are predicted to sense and respond to environmental stimuli that are specific to the site and circumstances of infection. How CsrRS repression of multiple virulence factors is beneficial to GAS survival and propagation within its host is not immediately clear, as *ΔcsrRS* strains are more virulent than the wild-type strain in skin infection models (Levin and Wessels, 1998; Heath *et al*., 1999). We recently made two observations that may point to a possible explanation for this phenomenon (Engleberg *et al*., 2001). First, spontaneous *csrRS* mutations occur *in vivo*, which greatly enhance dermonecrosis and the frequency of bacteraemia in a mouse model of skin and soft-tissue infection. These isolates usually represent a relatively small proportion of the total streptococci present. Secondly, in mixed inoculation experiments, the mutant subpopulation facilitates the growth of the wild-type strain *in vivo*, demonstrating a type of pathogenic synergy. These two observations suggest that the hypermutability of *csrRS* may be selectively advantageous for GAS, in that the presence of a small amount of spontaneous *csrRS* mutant facilitates the growth and transmission of the parental genotype (which retains the potential to generate more spontaneous mutants) to the next host.

Experimental procedures

Bacterial strains and plasmids

The wild-type strain of *S. pyogenes* used for PCR amplification was MGAS166 (Musser *et al*., 1993). This strain and its

Table 2. Oligonucleotides used in this study (excluding those shown in Fig. 7).

Name	Sequence	Use
csrRhisfor	5′-GATCGGATCCATGACAAAAGAAAATTTTA-3′	Create his-tagged CsrR
csrRhisrev	5′-GATCGGATCCTTATTTCTCACGAATAAC-3′	Create his-tagged CsrR
PcsrRfor1	5′-GATCGGATCCCCGCTACAGGTCTTGAC-3′	EMSA
PcrsRrev1	5′-GATCGGATCCCAACCCTTATTCTC-3′	EMSA, PE
PcsrRfor2	5′-GGTAATGACTATTTGATGCTTC-3′	EMSA
PcsrRrev2	5′-CCCTCATGTTGCAGCTCAAGAG-3′	EMSA, PE
PcsrRfor3	5′-GATTTAATCCTGCTTGACTTAATGTTACC-3′	EMSA
PcsrRrev3	5′-CGGGCAAGTAGTTCTTCAATGGC-3	EMSA
PcsrRintfor	5′-GCCATTGAAGAACTACTTGCCCG-3′	EMSA
PcsrRintrev	5′-CGTATCCCATGCCACGCACTG-3′	EMSA
PhasAfor	5′-CGATGGATCCCTATGACTAGTTGAC-3′	EMSA
PhasArev	5′-GATCGAATTCCCTACAGTTGATGTTCC-3′	EMSA, PE, footprint
Pskafor	5′-CACACACGTGCGGCTTGTTATCAGCACG-3′	EMSA
Pskarev	5′-GCTCCTAAAAGTTAAGTTTCAATCCCC-3′	EMSA, PE, footprint
PspeB1for	5′-GATCGGATCCCCGTATCCATATC-3′	EMSA, footprint
PspeB1rev	5′-GGTGAAAACCGTTGAATTCATTAGGC-3′	EMSA, PE, footprint
PspeB2rev	5′-CTATCGCATCTGGCTATG-3′	PE
PspeB3rev	5′-CCACATAGTAGGCGCCTCC-3′	PE
PspeB4rev	5′-GGGTTGTCATTGTTGACTCG-3′	PE
PspeB5rev	5′-CATCTGATGTGAGCCTAATTGG-3′	PE
PspeB6rev	5′-GGGTTAGCAAGAACAAATCCACC-3′	PE
PspeMFfor	5′-GATCGGATCCGACTACTGAGATCCCCTAC-3′	EMSA, footprint
PspeMFrev	5′-GCGCGAATTCCCGTCTTGATCCAAGTAGA-3′	EMSA, PE, footprint
Pctxfor	5′-GGCCGCTCTAGAACTAGTA-3′	EMSA, footprint
Pctxrev	5′-TCGACGGTATCGATAAGCTTG-3′	EMSA, footprint

Note that some oligonucleotides include restriction sites (underlined, with 4 bp flanking sequence) that are not found in GAS genomic sequence.

mucoid derivative, *ΔcsrRS*$^{-}$, which contains an internal deletion in the *csrR* coding region and a point mutation in the start codon (ATG to ACG) of *csrS* (Heath *et al*., 1999), were used for RNA isolation at various times throughout the growth curve. Overexpression for purification of his_6-CsrR was performed in the *E. coli* strain M15 supplied by Qiagen.

RNA isolation and primer extension analysis

Overnight cultures of MGAS166 wild-type and *ΔcsrRS*$^{-}$ strains were grown to various ODs in Todd–Hewitt broth (Difco) containing 2% yeast extract (Difco). Cultures were centrifuged, and total RNA was extracted from the resulting pellets using Bio101 FastRNA Blue purification kits and a Fastprep machine from Bio101. γ^{32}P end-labelled oligonucleotides ($\approx 1 \times 10^6$ c.p.m.) that mapped 3′ to the transcription start site (see Table 2) were annealed to 10 μg of RNA in 30 μl of hybridization buffer (80% Dl formamide, 40 mM PIPES, pH 6.4, 0.4 M NaCl, 1 mM EDTA) by heating at 80°C for 10 min, then incubating at 30°C for 2 h. After reprecipitation with EtOH, the RNA–annealed probe pellet was resuspended in 20 μl of reverse transcriptase mix [25 mM Tris, pH 8.3, 75 mM KCl, 3 mM $MgCl_2$, 5 mM dithiothreitol (DTT), 200 μM dNTPs, 10 U of RNasin (Gibco BRL)] and incubated with 50 U of Superscript II RNase H^{-} reverse transcriptase (Gibco BRL) at 48°C for 90 min. RNase A and EDTA were added to 100 μg ml^{-1} and 25 mM final concentrations, respectively, and the mixture was incubated for 30 min at 37°C. The samples were extracted once with phenol–chloroform, EtOH precipitated and resuspended in 100mM Tris/10 mM EDTA pH 8.0 (TE). Samples were analysed on a 6% sequencing gel followed by autoradiography.

Generation of PCR promoter fragments

Standard PCR amplification techniques were used. The oligos used for PCR amplification are listed in Table 2. For EMSA, the PCR products were end labelled with [γ^{32}P]-ATP (Amersham) and 10 U of T4 kinase (Gibco BRL) in 70 mM Tris, pH 6.4, 10 mM $MgCl_2$, 5 mM DTT for 30 min at 37°C; labelled probe was purified away from free nucleotide by passage over a G-25 spin column (Roche). To generate probes that were labelled on only one strand, PCR was performed as above, with the exception that one of the oligonucleotides was previously radiolabelled with [γ^{32}P]-ATP. These radioactive PCR products were purified on a native 6% polyacrylamide gel; radioactive probes were eluted in 0.5 M $NH_4CH_3CO_2H$, 1 mM EDTA, 0.1% SDS, ethanol precipitated twice and resuspended in ddH_2O before use.

Semi-exponential cycle sequencing

We followed the protocol of Sarkar and Bolander (1997) for semi-exponential cycle sequencing (SECS) except that the final dNTP concentration in the reaction mix was 4 μM, and all ddNTPs were at a final concentration of 200 μM.

Purification of his_6-CsrR

A his_6-tagged version of CsrR was created as follows: PCR amplification of the CsrR coding sequence using oligos csrRhisfor and csrRhisrev (see Table 2) was performed on the wild-type strain MGAS166. This PCR fragment was cloned into the *Bam*HI site of pQE30 from Qiagen. The resulting clone, pQE30-his_6csrR, was transformed into the M15 strain bearing the plasmid encoding the lac repressor, pREP4, according to the manufacturer's instructions (Qiagen). Cultures were grown up to an OD_{600} of 0.4 in LB containing 100 μg ml^{-1} ampicillin and 30 μg ml^{-1} kanamycin at 37°C, and his_6-CsrR expression was induced by the addition of IPTG to 0.5 mM. Bacteria were harvested by centrifugation at 6000 r.p.m. after 6 h, the pellet was resuspended in lysis buffer [50 mM NaH_2PO_4, 0.5 M NaCl, 10 mM EDTA, 0.5 mM phenylmethylsulphonyl fluoride (PMSF), 0.5% Tween 20; 4 ml g^{-1} pellet], lysozyme was added to a final concentration of 1 mg ml^{-1} and the suspension was incubated on ice for 30 min. The sample was subjected to six rounds of freeze–thaw (5 min each in a dry ice–EtOH bath and a 37°C water bath), then centrifuged at 10 000 r.p.m. for 30 min at 4°C. Supernatant from the spin was passed over Ni^{2+}-NTA agarose, which was then washed with five column volumes of lysis buffer; purified his_6-CsrR was eluted with lysis buffer + 250 mM imidazole. Purified protein was dialysed against storage buffer [50 mM Tris, pH 8.0, 100 mM NaCl, 1 mM EDTA ± 20% glycerol (depending on whether or not it was to be used for $OH^{\bullet}$ footprinting experiments, because $OH^{\bullet}$ cleavage will not occur in the presence of glycerol)] and stored at 4°C. All purified CsrR samples were cleared by centrifugation at 4°C for 1 min at 14 000 r.p.m. immediately before use in all experiments, thereby removing any possible aggregate contamination.

In vitro *phosphorylation of CsrR*

Purified his_6-CsrR was allowed to autophosphorylate in the presence of acetyl phosphate as follows: 0.1–2.4 μg of purified protein was incubated for 90 min at 37°C in freshly made phosphorylation buffer (20 mM NaH_2PO_4, pH 8.0, 10 mM $MgCl_2$, 1 mM DTT) with acetyl phosphate added to a final concentration of 32 mM. When applicable, this mixture was then used directly in the EMSA and footprinting analyses. Phosphorylation of CsrR using radiolabelled phosphate was performed according to the method of Quon *et al*. (1996).

Electrophoretic mobility shift assay (EMSA)

Varying concentrations of his_6-CsrR (0.3–2.4 μg corresponding to ≈ 0.75–6 μM) were incubated in freshly made DNA binding buffer [25 mM Tris, pH 8.0, 50 mM KCl, 0.5 mM EDTA, 0.5 mM DTT, 5 mM $MgCl_2$, 3 mM $CaCl_2$, 4% glycerol, 1 mg ml^{-1} BSA, 10 μg ml^{-1} salmon sperm DNA (Gibco BRL)] in a final volume of 15 μl at room temperature for 20 min with 10 000 c.p.m. of radiolabelled PCR fragments bearing the promoter elements of the desired genes, which were created as described above. Samples were analysed by native gel electrophoresis on 6% 0.5× TBE gels run at 4°C. In

the competition assays, cold competitor DNA at 100-fold excess was mixed with non-phosphorylated or phosphorylated his_6-CsrR in DNA binding buffer and incubated for 10 min before adding radioactive probes and proceeding as above. For these experiments, specific competitor was the same DNA as the labelled probe; non-specific competitor was AT-rich promoter DNA from the cholera toxin (*ctxA*) gene of *V. cholerae*.

DNase I footprinting

A sample of 9.6 μg of his_6-CsrR (12 μM) was incubated with 30 000 c.p.m. of the desired probe in a total volume of 30 μl under the same conditions as for the EMSA (see above). One microlitre of DNase I (Roche; 10 U μl^{-1}) at a dilution of 1:250 was added, and the mixture was incubated at room temperature for 2 min; then, the digestion was stopped with 200 μl of stop solution (200 mM NaCl, 2 mM EDTA, 1% SDS). The mixture was extracted once with phenol–chloroform, EtOH precipitated in the presence of 1 μl of glycogen (20 mg ml^{-1}) and resuspended in TE. Samples were analysed on a 6% sequencing gel followed by autoradiography.

$OH^{\bullet}$ footprinting

A sample of 9.6 μg of his_6-CsrR (12 μM) was incubated with 30 000 c.p.m. of the desired probe in a total volume of 30 μl in freshly made $OH^{\bullet}$ binding buffer [25 mM NaH_2PO_4, pH 8.0, 50 mM KCl, 0.5 mM EDTA, 0.5 mM DTT, 1 mg ml^{-1} BSA, 10 μg ml^{-1} salmon sperm DNA (Gibco BRL)] for 20 min at room temperature. Hydroxyl radical cleavage was performed according to the method of Tulius *et al.* (1987) by the addition of 3 μl of a freshly made Fe(II)-EDTA solution {made by dissolving [$(NH_4)_2Fe(SO_4)_2{\cdot}6H_2O$] (Sigma) to 8 mM and adding EDTA (pH 8.0) to 4 mM in H_2O} followed by 1.5 μl of 20 mM sodium ascorbate, then 1.5 μl of fresh 4.8% H_2O_2. The reaction was mixed well, incubated for 2 min at room temperature, then stopped by the addition of 3 μl of stop solution (0.1 M EDTA, 50 mM thiourea, 150 μg ml^{-1} yeast tRNA). TE was added to 250 μl, and the samples were then treated exactly as those for DNase I footprinting.

Gel filtration analysis

A sample of 150 μg of phosphorylated or non-phosphorylated his_6-CsrR (in 200 μl total volume) was loaded onto a 190 ml Biogel A-0.2M column equilibrated in 0.1 M NaCl, 50 mM Tris, pH 7.5 that had been prestandardized using a protein mixture (Sigma) consisting of the following: cytochrome *c* oxidase (12.9 kDa), carbonic anhydrase (29 kDa), BSA (66 kDa), alcohol dehydrogenase (150 kDa), β-amylase (200 kDa) and blue dextran (2 MDa). Fractions (2.7 ml) were collected at a flow rate of 1 ml min^{-1}. Each his_6-CsrR fraction (100 μl) was TCA precipitated and analysed by Coomassie-stained SDS–PAGE. Bands were quantified by NIH IMAGE 1.62 software and plotted against elution time as seen in Fig. 8B.

Acknowledgements

We would like to thank Alex Ninfa and his laboratory members for the use of chromatographic equipment, and Eric Krukonis, Dave Hendrixson and Phoebe Johnson for their thoughtful comments on the manuscript. A.A.M. is funded by National Research Service Award F32GM20420-01. This work was supported in part by PHS NIH grant AI 416482.

References

Alouf, J.E., and Loridan, C. (1988) Production, purification and assay of streptolysin S. *Methods Enzymol* **165**: 5–64.

Alouf, J.E., and Muller-Alouf, H. (1996) Cellular constituents and extracellular proteins involved in the pathogenic capacity of streptococcus group A. *Ann Pharm Fr* **54**: 49–59.

Ashbaugh, C., Warren, H., Carey, V., and Wessels, M. (1998) Molecular analysis of the role of the group A streptococcal cysteine protease, hyaluronic acid capsule, and M protein in a murine model of human invasive soft-tissue infection. *J Clin Invest* **102**: 550–560.

Atlung, T., and Ingmer, H. (1998) H-NS: a modulator of environmentally regulated gene expression. *Mol Microbiol* **24**: 7–17.

Bernish, B., and van de Rijn, I. (1999) Characterization of a two-component system in *Streptococcus pyogene*s which is involved in regulation of hyaluronic acid production. *J Biol Chem* **274**: 4786–4793.

Betschel, S.D., Borgia, S.M., Barg, N.L., Low, D.E., and DeAzavedo, J.C. (1998) Reduced virulence of group A streptococcal Tn916 mutants that do not produce streptolysin S. *Infect Immun* **66**: 1671–1679.

Caparon, M.G., and Scott, J.R. (1987) Identification of a gene that regulates expression of M protein, the major virulence determinant of group A streptococci. *Proc Natl Acad Sci USA* **84**: 8677–8681.

Chaussee, M.S., Gerlach, D., Yu, C.E., and Feretti, J.J. (1993) Inactivation of the streptococcal pyrogenic erythrogenic toxin B gene (*speB*) in *Streptococcus pyogenes*. *Infect Immun* **61**: 3719–3723.

Chaussee, M.S., Phillips, E.R., and Ferretti, J.J. (1997) Temporal production of streptococcal erythrogenic toxin B (streptococcal cysteine proteinase) in response to nutrient depletion. *Infect Immun* **65**: 1956–1959.

Chaussee, M.S., Adjic, D., and Ferretti, J.J. (1999) The *rgg* gene of *Streptococcus pyogenes* NZ131 positively influences extracellular SpeB production. *Infect Immun* **67**: 1715–1722.

Cotter, P.A., and DiRita, V.J. (2000) Bacterial virulence gene regulation: an evolutionary perspective. *Annu Rev Microbiol* **54**: 519–565.

Cunningham, M.W. (2000) Pathogenesis of group A streptococcal infections. *Clin Microbiol* **13**: 470–511.

Dahl, J.L., Wei, B.Y., and Kadner, R.J. (1997) Protein phosphorylation affects binding of the *E. coli* transcription activator UhpA to the *uhpT* promoter. *J Biol Chem* **272**: 1910–1919.

Dougherty, B.A., and van de Rijn, I. (1994) Molecular

characterization of *hasA* from an operon required for hyaluronic acid synthesis in group A streptococci. *J Biol Chem* **269**: 169–175.

Drew, H.R., and Travers, A.A. (1984) DNA structural variations in the *E. coli tyrT* promoter. *Cell* **37**: 491–502.

Egger, L.A., Park, H., and Inouye, M. (1997) Signal transduction via the histidyl-aspartyl phosphorelay. *Genes Cells* **2**: 167–184.

Engleberg, N.C., Heath, A.S., Miller, A.A., Rivera, C., and DiRita, V.J. (2001) Spontaneous mutations in the CsrRS two-component regulatory system of *Streptococcus pyogenes* result in enhanced virulence in a murine model of skin and soft tissue infection. *J Infect Dis* **183:** 1043–1054.

Federle, M.J., McIver, K.S., and Scott, J.R. (1999) A response regulator that represses transcription of several virulence operons in the group A *Streptococcus*. *J Bacteriol* **181**: 3649–3657.

Feingold, D.S., and Weinburg, A.N. (1996) Group A streptococcal infections: an old adversary reemerging with new tricks? *Arch Dermatol* **132**: 67–70.

Fogg, G., Gibson, C., and Caparon, M. (1994) The identification of *rofA*, a positive-acting regulatory component of *prtF* expression: use of an m gamma delta-based shuttle mutagenesis strategy in *Streptococcus pyogenes*. *Mol Microbiol* **11**: 671–684.

Forst, S., Delgado, J., and Inouye, M. (1989) Phosphorylation of OmpR by the osmosensor EnvZ modulates expression of the *ompF* and *ompC* genes in *E. coli*. *Proc Natl Acad Sci* **86**: 6052–6056.

Galinier, A., Garnerone, J.M., Reyrat, D., Kahn, J., Batut, J., and Boistard, P. (1994) Phosphorylation of the *Rhizobium meliloti* FixJ protein induces its binding to a compound regulatory region at the *fixK* promoter. *J Biol Chem* **269**: 23784–23789.

Heath, A., DiRita, V.J., Barg, N.L., and Engleberg, N.C. (1999) A two-component regulatory system, CsrR-CsrS, represses expression of three *Streptococcus pyogenes* virulence factors: hyaluronic acid capsule, streptolysin S and pyrogenic exotoxin B. *Infect Immun* **67**: 5298–5305.

Hess, J.F., Oosawa, K., Kaplan, N., and Simon, M.I. (1988) Phosphorylation of three proteins in the signaling pathway of bacterial chemotaxis. *Cell* **53**: 79–87.

Hoch, J.A., and Silhavy, T.J. (1995) *Two-Component Signal Transduction.* Washington, DC: American Society for Microbiology Press.

Kaplan, E.L. (1996) Recent epidemiology of group A streptococcal infections in North America and abroad: an overview. *Pediatrics* **97**: 945–948.

Karimova, G., Gellalou, J., and Ullmann, A. (1996) Phosphorylation-dependent binding of BvgA to the upstream region of the *cyaA* gene of *Bordetella pertussis*. *Mol Microbiol* **20**: 489–496.

Kuo, C.F., Wu, J.J., Lin, K.Y., Tsai, P.J., Lee, S.C., Jin, Y.T., *et al.* (1998) Role of streptococcal pyrogenic exotoxin B in the mouse model of group A streptococcal infection. *Infect Immun* **66**: 3931–3935.

Levin, J.C., and Wessels, M.R. (1998) Identification of *csrR/csrS*, a genetic locus that regulates hyaluronic acid capsule synthesis in group A *Streptococcus*. *Mol Microbiol* **30**: 209–219.

Li, Z., Sledjeski, D.D., Kreikemeyer, B., Podbielski, A., and Boyle, M.D. (1999) Identification of *pel*, a *Streptococcus pyogenes* locus that affects both surface and secreted proteins. *J Bacteriol* **181**: 6019–6027.

Lottenberg, R., DesJardin, L.E., Wang, H., and Boyle, M.D. (1992) Streptokinase-producing streptococci grown in human plasma acquire unregulated cell-associated plasmin activity. *J Infect Dis* **166**: 436–440.

Lukomski, S., Sreevatsan, S., Amberg, C., Reichardt, W., Woischnik, M., Podbielski, A., and Musser, J.M. (1997) Inactivation of *Streptococcal pyogenes* extracellular cysteine protease significantly decreases mouse lethality of serotype M3 and M49 strains. *J Clin Invest* **99**: 2574–2580.

Lyon, W.R., Gibson, C.M., and Caparon, M.G. (1998) A role for Trigger factor and an Rgg-like regulator in the transcription, secretion and processing of the cysteine proteinase of *Streptococcus pyogenes*. *EMBO J* **17**: 6263–6275.

McIver, K.S., Thurman, A.S., and Scott, J.R. (1999) Regulation of *mga* transcription in the group A streptococcus: specific binding of Mga within its own promoter and evidence for a negative regulator. *J Bacteriol* **181**: 5373–5383.

Moses, A.E., Wessels, M.R., Zalcman, K., Alberti, S., Natanson-Yaron, S., Menes, T., and Hanski, E. (1997) Relative contributions of hyaluronic acid capsule and M protein to virulence in a mucoid strain of the group A *Streptococcus*. *Infect Immun* **65**: 64–71.

Musser, J., Kanjilal, S., Shah, U., Msher, D., Barg, N., Nelson, K., *et al.* (1993) Geographic and temporal distribution and molecular characterization of two highly pathogenic clones of *Streptococcus pyogenes* expressing allelic variants of pyrogenic exotoxin A (scarlet fever toxin). *J Infect Dis* **167**: 337–346.

Musser, J.M., Stockbauer, K., Kapur, V., and Rudgers, G.W. (1996) Substitution of cysteine 192 in a highly conserved *Streptococcus pyogenes* extracellular cysteine protease (interleukin 1 convertase) alters proteolytic activity and ablates zymogen processing. *Infect Immun* **64**: 1913–1917.

Ohara-Nemoto, Y., Sasaki, M., Kaneko, M., Nemoto, T., and Ota, M. (1994) Cysteine protease activity of streptococcal pyrogenic exotoxin B. *Can J Microbiol* **40**: 930–936.

Perez-Martin, J., and de Lorenzo, V. (1997) Clues and consequences of DNA bending in transcription. *Annu Rev Microbiol* **51**: 593–628.

Podbielski, A., Woischnik, M., and Schmidt, K. (1996) What is the size of the group A streptococcal vir regulon? The Mga regulator affects expression of secreted and surface virulence factors. *Med Microbiol Immunol* **185**: 171–181.

Podbielski, A., Wioschnik, M., Leonard, B., and Schmidt, K.H. (1999a) Characterization of *nra*, a global negative regulator gene in group A streptococci. *Mol Microbiol* **31**: 1051–1064.

Podbielski, A., Woischnik, M., Kreikemeyer, B., Bettenborck, K., and Buttaro, B.A. (1999b) Cysteine protease SpeB in group A streptococci is influenced by the nutritional environment but does not contribute to obtaining essential nutrients. *Med Microbiol Immunol* **188**: 99–109.

Quon, K.C., Marczynski, G.T., and Shapiro, L. (1996) Cell cycle control by an essential bacterial two-component signal transduction protein. *Cell* **84**: 83–93.

Sarkar, G., and Bolander, M. (1997) Direct sequencing of

unpurified PCR-amplified DNA by semi-exponential cycle sequencing (SECS). *Mol Biotech* **8**: 269–277.

Schlievert, P.M., Assimacopoulos, A.P., and Cleary, P.P. (1996) Severe invasive group A streptococcal disease: clinical description and mechanisms of pathogenesis. *J Lab Clin Med* **127**: 13–22.

Spurio, R., Falconi, M., Brandi, A., Pon, C.L., and Gualerzi, C.O. (1997) The oligomeric structure of nucleoid protein H-NS is necessary for recognition of intrinsically curved DNA and for DNA bending. *EMBO J* **16**: 1795–1805.

Sriskandan, S., Unnikrishnan, M., Krausz, T., and Cohen, J. (2000) Mitogenic factor (MF) is the major DNase of serotype M89 *streptococcus pyogenes*. *Microbiology* **146**: 2785–2792.

Stevens, D.L. (1992) Invasive group A streptococcus infections. *Clin Infect Dis* **14**: 2–13.

Tulius, T.D., Dombroski, B.A., Churchill, M.A.E., and Kam, L. (1987) Hydroxyl radical footprinting: a high resolution method for mapping protein-DNA contacts. *Methods Enzymol* **155**: 537–558.

Unnikrishnan, M., Cohen, J., and Sriskandan, S. (1999) Growth-phase-dependent expression of virulence factors in an M1T1 clinical isolate of *Streptococcus pyogenes*. *Infect Immun* **67**: 5495–5499.

Weiss, V., and Magasanik, B. (1988) Phosphorylation of nitrogen regulator I (NRI) of *Escherichia coli*. *Proc Natl Acad Sci USA* **85**: 8919–8923.

Wessels, M.R., and Bronze, M.S. (1994) Critical role of the group A streptococcal capsule in pharyngeal colonization and infection in mice. *Proc Natl Acad Sci USA* **91**: 12238–12242.

Williams, R.M., and Rimsky, S. (1997) Molecular aspects of the *E. coli* nucleoid protein, H-NS: a central controller of gene regulatory networks. *FEMS Microbiol Lett* **156**: 175–185.

Wu, H.M., and Crothers, D.M. (1984) The locus of sequence-directed and protein-induced DNA bending. *Nature* **308**: 509–513.

Yutsudo, T., Murai, H., Gonzalez, T., Takao, Y., Shimnishi, Y., Takeda, Y., *et al.* (1992) A new type of mitogenic factor produced by *Streptococcus pyogenes*. *FEBS Lett* **308**: 30–34.